Climate Dynamics (2002) 18: 369–381
DOI 10.1007/s003820100182

R. Bojariu · G. Reverdin

Large-scale variability modes of freshwater flux and precipitation over the Atlantic

Received: 10 February 2000 / Accepted: 7 May 2001

Abstract Precipitation (P) and freshwater (E-P) fluxes at the air-sea interface are investigated in the Atlantic Ocean sector using the reanalyses of the European Centre for Medium Range Weather Forecasts (ERA) and of the National Centers for Environmental Prediction (NCEP). A canonical correlation analysis method between these fields and sea level pressure (SLP) is used to identify patterns. We also test whether precipitation and freshwater fluxes can be reconstructed from SLP data. In the winter months, patterns associated with both the North Atlantic Oscillation (NAO) and the East Atlantic (EA) mode are identified. The signals are strong enough to be reconstructed from the reanalysis fields, and they correspond to a significant part of the variability. The NAO signal is more robust than the EA one. The NAO-related variability mode is also present when the monthly precipitation rate is averaged for the winter season and even for annual averages. However, in the later case, other variability of natural origin (for instance, ENSO variability) or noise from the model and assimilation system prevents the reconstruction of E-P associated with NAO from SLP variability. Difficulties are identified in the tropical Atlantic with a different behaviour of NCEP and ERA precipitation variability, especially near the Inter Tropical Convergence Zone (ITCZ). The ERA patterns suggest a NAO signature in the tropical Atlantic which has clear monthly patterns and indicates a link between the phase of NAO and changes in the position and intensity of ITCZ. However, the analysis of winter rainfall based on satellite and in situ data does not support the monthly tropical pattern of ERA precipitation although it suggests a relation between convection near 15°S and NAO during northern winter.

R. Bojariu
National Institute of Meteorology and Hydrology,
Sos. Bucuresti-Ploiesti no. 97, Bucuresti, Romania

G. Reverdin (✉)
Laboratoire d'Etudes en Géodésie et Océanographie Spatiale,
14 Av. E. Belin, 31401 Toulouse Cx4, France

1 Introduction

Much is known about air-sea heat exchanges and their effect on the atmosphere and ocean. For instance, a large portion of the sea surface temperature (SST) variability can be understood as a response to the air-sea heat fluxes with much of the latent heat associated with evaporation (e.g. Frankignoul et al. 1998; Halliwell 1998; Seager et al. 1999). It has been suggested that subtropical and mid-latitude SSTs are influencing the midlatitude atmospheric variability through atmospheric heating processes in which evaporation and precipitation are important factors (Palmer and Sun 1985; Rodwell et al. 1999).

Changes in the air-sea freshwater flux affect salinity, and therefore the upper ocean layer density and stratification. Net freshwater fluxes over the whole North Atlantic have been shown in model studies to have an influence on the thermohaline circulation if they last long enough (Rahmstorf 1995). A change of this flux has been shown to happen during El Niño events (for example, Schmittner et al. 1999). Large changes in the stratification have been found in the upper surface layers of the subpolar gyre (Dickson et al. 1988; Lazier 1995; Curry et al. 1998). Model studies suggest that this could result in changes in the formation rate of deep water and therefore could affect the strength of Atlantic meridional overturning circulation (MOC) (Mauritzen and Häkkinen 1997; Häkkinen 1999a), and indirectly the distribution of SST. It is not clear to what extent changes in the air-sea freshwater fluxes have contributed to these changes and to the variability of the observed surface salinity changes in the subpolar gyre.

Having a good estimate of the freshwater exchanges at the air-sea interface and of their relation to the atmospheric modes of variability would therefore contribute to a better understanding of the variability of the North Atlantic. Cayan (1992) has found that the evaporation over the Atlantic is related to both North Atlantic Oscillation (NAO) and Eastern Atlantic (EA) modes. NAO is the dominant mode of variability in the

North Atlantic sector throughout the year, although it is most pronounced during winter. The phenomenon has been defined in the sea level pressure (SLP) anomaly field as a dipole-like structure with centres of action near the Icelandic low and the Azores high (e.g. Walker and Bliss 1932; van Loon and Rogers 1978). Complementary changes in westerlies over the North Atlantic and in trades over the tropical Atlantic together with heat flux and sea surface temperature anomalies characterize the two NAO phases (Cayan 1992; Wallace et al. 1990). The Eastern Atlantic pattern is the second of the dominant modes of low frequency variability over the North Atlantic, appearing in all months except May–August. The main SLP anomaly centre in the EA pattern is situated over the mid latitude regions, between the two NAO variability centres. A lower latitude EA centre is also present showing a connection with the subtropical ridge (Barnston and Livezey 1987).

However the large-scale features of freshwater exchange and precipitation at the ocean surface are still rather uncertain over the Atlantic. There is some evidence from data that NAO is associated with distinctive patterns of precipitation and freshwater fluxes (Cayan and Reverdin 1994). According to meteorological forecast model analyses and reanalyses, the two opposing NAO phases strongly affect the winter temperature and precipitation conditions over the Atlantic sector and the nearby continental areas from monthly to decadal time scales (Hurrell 1995; Hurrell and van Loon 1997; Dai et al. 1997). The composite plots of vertically integrated moisture transport in (Hurrell 1995) show that during high NAO index intervals the axis of moisture transport shifts to a more southwest to northeast orientation across the Atlantic and extends towards northern Europe and Scandinavia. A significant reduction of the total atmospheric transport occurs towards southern Europe and North Africa. Atmospheric general circulation models (AGCM) forced by specified SST anomalies also display changes of the precipitation patterns. In Palmer and Sun (1985), in response to SST anomalies in the northwestern Atlantic, the main precipitation anomalies were over the area of forcing. In Rodwell et al.'s (1999) response to observed SST distribution, the precipitation response that is associated with an atmospheric mode resembling NAO is also mostly over the area of the largest SST anomalies.

Our main goals here are firstly to relate the large-scale variability of the freshwater flux (E-P) and precipitation over the North Atlantic Ocean to known patterns of atmospheric circulation, and secondly to test whether freshwater flux and precipitation can be reconstructed over a longer period, based on better-known time series of dominant atmospheric variability. The main emphasis is from the subtropics to the high latitudes, and tropical modes of variability will be identified only to the extent that they are related to extra-tropical variability. The data sets used have known flaws in the tropics or are not long enough for the investigation. Also, in the tropics, the variability is influenced by external forcing, in particular by ENSO, with large associated signals in rainfall near northern South America and in the Gulf of Mexico, where it explains more than 10% of the winter variance according to a linear regression on the Niño3 equatorial Pacific temperature index (see also Giannini et al. 2000; Ropelewski and Halpert 1996, for studies on this subject in the Atlantic sector). However, this large ENSO-related variability corresponds only to a small part of the spatially integrated variance at subtropical and higher latitudes.

Global reanalyses made at the European Centre for Medium-Range Weather Forecasts (ECMWF) and at the National Centers for Environmental Prediction/National Center for Atmospheric Research (NCEP/NCAR, that we will refer to as NCEP) are now available that can provide the temporal and spatial variability of freshwater fluxes (Kalnay et al. 1996; Gibson et al. 1997). Canonical correlation analysis (CCA) is used to identify the related patterns of freshwater flux, precipitation and SLP anomalies. The identified canonical correlation modes are further used to build a multiple regression model for the reconstruction of E-P and precipitation variability from SLP data. Among other statistical techniques used to analyze coupled variability modes, the CCA has the advantage of finding coupled spatial patterns best correlated in time for the multiple regression model.

2 Data

In the present study, monthly rates of precipitation and evaporation for the domain 90°W to 30°E and from 30°S to 90°N are extracted from the re-analyses of the European Centre for Medium Range Weather Forecasts (ECMWF) and of the National Centers for Environmental Predictions (NCEP). The two reanalyses products are used because they are based on somewhat different data and assimilation schemes, and provide therefore two different estimates of the actual variability. The common period is short (1979–1993), but proved sufficient for identifying patterns which can be checked in NCEP for a longer period (1957–1999), and validated by comparisons with data-based retrievals of the precipitation (either from ship reports or satellite data; see the discussion section). Monthly means of sea level pressure over the North Atlantic region are extracted from the NCEP reanalysis from 90°W to 30°E and from 0° to 90°N.

The NCEP reanalyses use a global data assimilation system which is kept unchanged over the period 1957 through 1999 (Kalnay et al. 1996). The NCEP reanalyses are not initialized because the statistical spectral interpolation eliminates imbalances in the initial state. The re-analysis incorporates all the data of the operational analyses enhanced with observations from aircraft, cloud winds, SSM/I winds after July 1987, and additional ship observations, as well as data from the special observation periods FGGE and Alpex. The NCEP precipitation and surface fluxes are derived from the model 6-h forecasts.

The ECMWF reanalysis (ERA) archive contains global analyses and short range forecasts of all relevant weather parameters obtained with an invariant and consistent data assimilation system which is kept unchanged over the interval 1979–1993. The data assimilation system is a special version of the operational data assimilation scheme and adiabatic nonlinear normal mode initialization. As in the NCEP reanalysis experiment, the data base has been enhanced with data not available when operational analyses were made, and in addition includes one-dimensional variational physical retrieval of TOVS cloud-cleared radiance data. The SST boundary conditions differ slightly from NCEP, but in both cases are based on in situ and satellite observations. The prognostic

cloud scheme developed by Tiedtke (1993) is used. Prognostic equations for cloud water and cloud cover are solved, and these quantities as well as specific humidity are advected in grid point space rather than in spectral space to avoid the problems due to spectral truncation. A comprehensive description is given in Gibson et al. (1997). In the present study we use data from ERA06 (6 h forecasts four times a day).

Stendel and Arpe (1997) have investigated the quality of the precipitation in different re-analyses products, based on comparisons with in situ and satellite retrievals of precipitation, both over the continents and the oceans, although the conclusions are mostly based on the comparisons over land. They show that, in general, for the actual amount of precipitation ERA24 (24-h forecast, twice a day) fits observations better than ERA06, but for temporal variability studies the use of ERA06 data is recommended, in particular for the winter season and over the subtropical regions. The study also reveals that the consistency of both NCEP and ERA reanalyses is better than in the operational analyses. However, in the tropics and extra-tropical summer, NCEP and ERA reanalyses overestimate the convective precipitation. Also, questionable trends of increasing precipitation over the tropical ocean are visible in ERA. Another problem was identified beginning around 1986–87 when it was discovered that the African ITCZ precipitation maximum shifted from north of the equator to a position just south of it. Kållberg (1997) describes a discrepancy in the precipitation and soil temperature and moisture in a limited area in the western equatorial Amazonia affecting the first eight years of ERA data, and stresses that detailed conclusions on the behaviour of the tropical convergence, particularly over South America and its associated precipitation patterns should be carefully drawn. We therefore expected large uncertainties in this study for the tropical areas. However, these problems did not affect the higher latitudes much, as we found by comparing results for the analyses of ERA and NCEP, which proved quite similar (see results in Sect. 4.).

We also use data sets to verify the results based on the reanalyses products for specific periods (see discussion section). Monthly rates of precipitation and evaporation estimated from the COADS data set of ship reports (Da Silva et al. 1994) are used for the comparison with the reanalyses in the interval 1976–1989. This period is known to be most consistent in the precipitation data with changes in reporting practices inducing large biases before and after (see also Cayan and Reverdin 1994). Other products, mostly based on satellite data over the oceans (the Global Precipitation Climatology Project, GPCP, for 1988–1998, Huffman et al. 1996, and the Xie and Arkin 1997, data set for 1979–1998) have also been used to validate the results for precipitation. GPCP is based on conventional and satellite measurements (Huffman et al. 1996). This product over the ocean is mostly derived from the satellite-derived precipitation using radiance measurements (GPI) and is considered reliable (Stendel and Arpe 1997). The composite product of Xie and Arkin (1997) is based on gauge and satellite data over the ocean and covers the years 1979 to 1998. (A blend with model outputs is made, with effects mostly north of 50°N.)

3 Methods

The freshwater flux (E-P) and precipitation from the reanalyses are analyzed using empirical orthogonal functions (EOF) and canonical correlation analysis (CCA). The EOF analysis makes an optimal representation of the covariance structure of a multicomponent data set and identifies patterns that maximize the explained variance (Preisendorfer 1988; von Storch 1995). The eigenvectors of the covariance matrix show the spatial structures of variability and the corresponding principal components describe the temporal behaviour of the data. The amount of variance covered by each eigenvector is obtained from the associated eigenvalues. The eigenvectors are orthogonal to one another and the principal components are uncorrelated.

The CCA selects a pair of spatial patterns of two variables such that their time evolution is optimally correlated (Preisendorfer 1988; Zorita et al. 1992; Bretherton 1992; von Storch and Frankignoul 1995). Before canonical correlation analysis the original data are usually projected onto their EOFs, retaining only a limited number of them in order to avoid noise. The canonical correlation tends to be overestimated if the number of EOFs is too large. Therefore, in building CCA modes we should take into account simultaneously the requirement of including a large share of the variance and the constraint regarding the noise from the data (Kharin 1994; von Storch 1995). The EOF and CCA patterns are normalized such that the coefficients have unit standard deviation, so the patterns represent typical anomalies in their specific units. For both EOF and CCA decomposition an uncertainty arises due to the limited sampling of the available data sets (von Storch and Frankignoul 1995; Bretherton et al. 1992).

The stability and robustness of the variability patterns in the freshwater flux and precipitation data from the reanalyses over the Atlantic are verified using a reconstruction technique. The technique has been proposed by von Storch et al. (1993) and used in many studies mainly for downscaling large scale climate signals to a regional level (e.g. Cui et al. 1995; Hauke et al. 1996; Busuioc et al. 1999). A subset of CCA pairs representing two fields is used in a regression model to estimate the anomalies of one variable from the anomalies of the other using the correlation coefficients between the corresponding time components. The performance of the model is sensitively dependent on the number of EOFs and CCA pairs used in the regression model. In this study the number of EOFs retained in the CCA and the number of CCA pairs used in the regression model have been determined simultaneously such that the skill of the model is highest. Here, the skill of the model is expressed by the correlation coefficients between principal components associated with the significant EOF modes of the original and reconstructed data because the present study is oriented towards signal detection.

The reconstruction is made to obtain freshwater flux and precipitation anomalies from the sea level pressure knowing that large-scale phenomena such as NAO are well represented in the SLP field, in particular during the winter season. By that choice, we tend to select modes of variability with a large signal at middle or high latitudes. An attempt has been made to identify large-scale variability features over the Atlantic using the linkage between precipitation and wind instead of precipitation and SLP. It was thought that this would help separate tropical modes of variability which have a large wind signal but a much weaker pressure signal than at higher latitudes. To some extent the results are similar to the ones when SLP is used but they are less robust, and will therefore not be presented.

Both ERA and NCEP data are used with SLP to train reconstruction models but using different time periods and time scales. Monthly, seasonal and annual means have been used as inputs in the EOF decomposition and CCA. The reconstruction based on a model for a given period is compared with the observations for an independent time interval. Also, the pattern stability is tested by splitting the independent time interval in two and comparing the simulated and observed patterns for the two subintervals. This is also a test of the consistency in time of the NCEP and ERA precipitation and freshwater fluxes. The length of the time series is often short, in particular for ERA. Therefore, the details in the patterns we find for specific intervals are not necessarily representative of longer time series. Other data products are used mostly to verify the patterns, which is approached by constructing regression or correlation patterns as well as by the same CCA method. Their short time series do not warrant a more sophisticated approach.

4 Results

4.1 NCEP P and E-P patterns

The variance patterns for precipitation and E-P in NCEP data revealed (not shown) that variability is larger in winter months than in summer outside the

tropics. Also, the spatial features are different in the warm and cold seasons. For mid-latitude regions during summer months, higher values for precipitation variance are found mainly in the southwestern part of the North Atlantic whereas during winter months high variance in precipitation is found over the midlatitude North Atlantic with a pattern corresponding to the average storm track.

The CCA analysis between the SLP and precipitation (or *E-P* flux) anomalies from the NCEP reanalysis was done for monthly averages in individual seasons. In general, the correlation coefficients corresponding to CCA modes of SLP, and freshwater flux for the winter months (December, January and February) are larger than for the summer months (June, July and August). The variance explained by the first CCA modes is larger in winter than in summer and large-scale features are more easily identified in winter. Therefore we will focus on the winter season.

The CCA analysis for the winter months produces two clearly identified large-scale modes in both the precipitation and *E-P* field. The two modes of freshwater flux and precipitation anomalies correspond to SLP patterns that resemble the North Atlantic Oscillation and East Atlantic mode, respectively Wallace and Gutzler (1981). (The associated time series are also highly correlated.) Figure 1 illustrates the CCA modes of SLP/precipitation and SLP/*E-P* respectively. (Seven EOFs were retained for SLP, *P* and *E-P*.) The correlation coefficients *R* and the portion of total variance explained by the first two CCA modes for SLP/precipitation and SLP/*E-P* pairs are quite large (Table 1).

The first CCA pattern for *P* (Fig. 1a) presents two variability centres with opposite signs offshore from southern Europe and from eastern Greenland to Scandinavia, which indicate a displacement of the precipitation consistent with changes of vertically integrated moisture transport shown by Hurrell (1995). This is related to changes in the position of the storm track and in the storm intensity according to the NAO phase (Rogers 1990). In the eastern Atlantic, this corresponds to a north-south dipole in precipitation. A similar displacement was found in the study of Cayan and Reverdin (1994) based on COADS data. The CCA precipitation pattern associated with the Eastern Atlantic mode (Fig. 1b) shows a main variability centre in the central North Atlantic near 50°N over the area of high variability in the associated SLP pattern, and anomalies of the opposite sign in the central Atlantic at 30–35°N where the SLP pattern reveals a secondary centre of action with opposing anomalies.

The spatial dipole pattern of SLP associated with precipitation for NAO is slightly shifted to the northeast of the SLP dipole position associated with *E-P* (Fig. 1a, c). Interestingly, the rainfall pattern related to NAO has no component in the western Atlantic, whereas the evaporation has a strong related variability in the western Atlantic (not shown, but indicated by the difference between *P* and *E-P* pattern in Fig. 1). It is in the western Atlantic that SST and air temperature variability associated with NAO is the largest, thus the strong loading of evaporation in the western Atlantic is reminiscent of the strong heat flux variability associated there with NAO (Cayan 1992). The *E-P* pattern is linked with a SLP dipole-like pattern with its north/south axis shifted towards the central region of North Atlantic compared with the SLP dipole farther east associated with the rainfall variability. These spatial differences in the SLP centres of action could be indicative of a combination in NAO of atmospheric dynamics and air-sea interactions. The area of largest heat flux and evaporation variability is located in the western Atlantic (Cayan 1992), whereas the low frequency teleconnections that are linked to the predominant mode of the storm track variability are in the far northeastern Atlantic (Rogers 1997). Opposite precipitation anomalies are found for CCA 1 between the southwestern and southeastern coast of Greenland which is likely to result from the orography.

An intriguing feature of the CCA precipitation pattern (Fig. 1a) is the presence of a variability centre in the subtropical Atlantic situated near 20°N. A similar signal shifted towards the western tropical Atlantic is also present in the EA related mode (Fig. 1b) and it is difficult to provide a physical interpretation of this feature. We have also performed canonical correlation analysis of precipitation with zonal and meridional wind components (not shown). In this case, no subtropical centre of variability was identified for the precipitation anomalies associated with NAO and EA. This suggests that caution is required in interpreting the variability in the western and central regions of the subtropical and tropical Atlantic. These regions are also strongly influenced by tropical modes of variability or ENSO, not directly related with NAO or EA, as was tested by regression to ENSO indices (see also Giannini et al. 2000 for a discussion relevant to the Caribbean area).

The NAO structure in the *E-P* field (Fig. 1c) shows negative anomalies in the region near the eastern US seaboard and in the northeastern Atlantic near the Scandinavian coast, and positive anomalies within a large area from the Labrador Sea and southern Greenland to the eastern subtropical Atlantic. The pattern can be explained by a combination of the precipitation of Fig. 1a and the evaporation which is stronger during a strong NAO in the northeastern Atlantic due to enhanced trades (Bojariu 1997) and over the Labrador Sea due to stronger northwesterly winds which advect dry air over the ocean. In the central regions of the North Atlantic, evaporation exceeds precipitation due to stronger westerlies, whereas the opposite holds off southern Europe. The *E-P* near-coastal structure off the eastern US seaboard is the result of the land/ocean contrast in winter. In the high NAO index case, warm and moist air is advected over the eastern coast causing positive precipitation and negative evaporation anomalies. The situation is reversed for a low NAO index. The *E-P* pattern related to the EA mode is represented by the

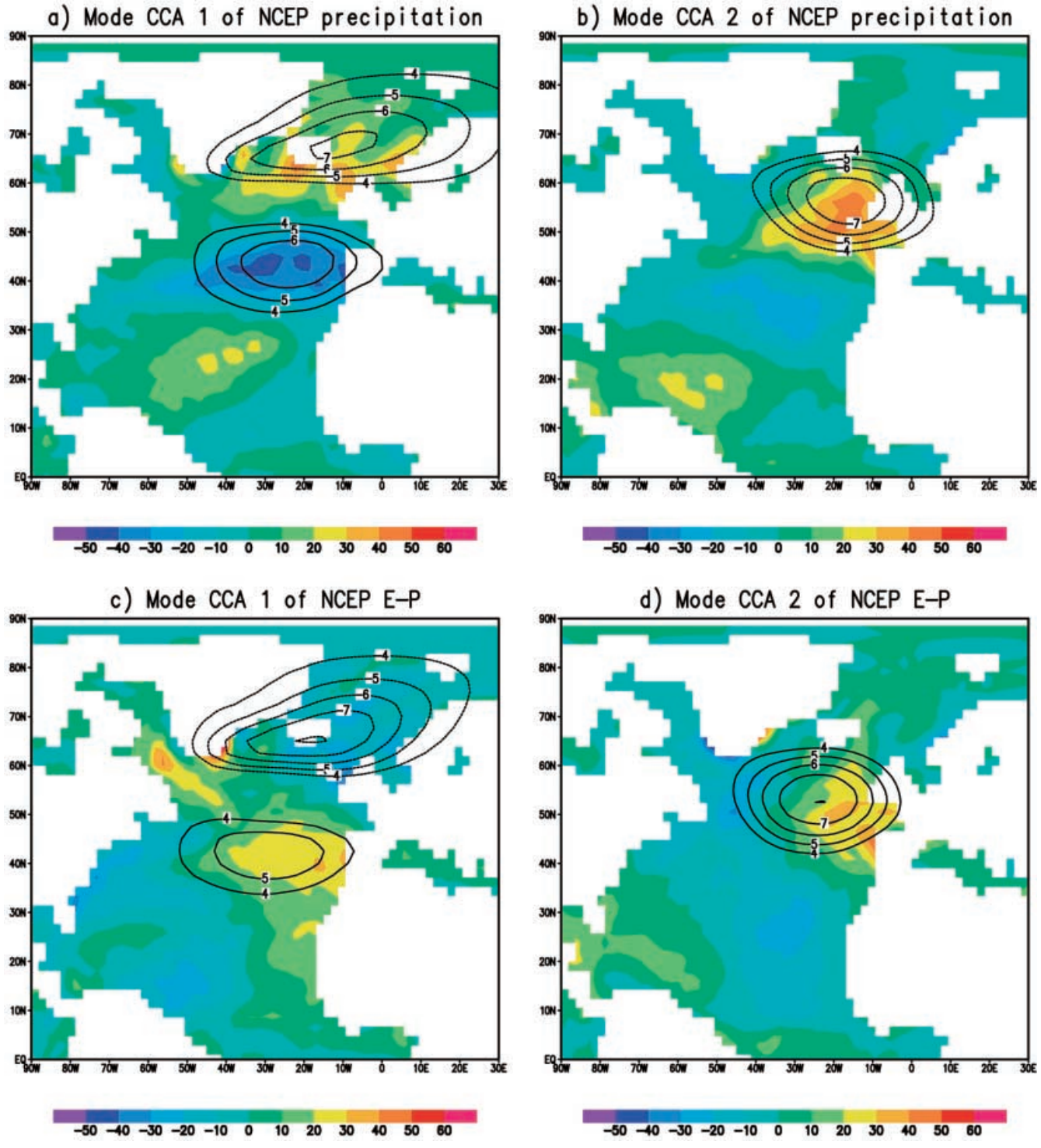

Fig. 1a–d Patterns of first and second CCA between P and SLP **a** and **b** and between E-P and SLP **c** and **d**. Contours for NCEP SLP (mb) and color plot for the associated NCEP precipitation and E-P (mm/month) patterns

second CCA (Fig. 1d) and is mainly governed by the precipitation signal over an area westward of Britain and Ireland. Wind effects related to land-ocean contrast in winter are also present near the Iberian coast.

The *E-P* and precipitation patterns of CCA modes presented show good agreement with other studies. Similar features are usually found in a winter *E-P* composite difference between the winters with high and low NAO index derived by Hurrell (1995) from the moisture budget in the ECMWF analyses. However, his composite map of *E-P* has a weak NAO related variability in the northeastern subtropical Atlantic, and Hurrell (1995) noticed that the computed *E-P* pattern is not supported by observed precipitation in this area.

Our analysis does not show such a disagreement. Cayan (1992) and Cayan and Reverdin (1994) have also found latent heat flux, precipitation and *E-P* patterns which indicate the control exerted by the two types of large-scale atmospheric circulation inferred from the SLP field over the North Atlantic. The patterns presented in their studies have been obtained using COADS data (Woodruff et al. 1987), but they are consistent with our results.

Table 1 CCA analysis results of *P*/SLP and of *E-P*/SLP from NCEP 1958–1999 winter months. For each pair, the correlation coefficients and variance explained are indicated for the first two pairs

CCA number	*R*	Variance of SLP(%)	Variance of *P*(%)	*R*	Variance of SLP(%)	Variance of *E-P*(%)
1	0.96	32	11	0.95	32	8
2	0.93	13	8	0.93	12	6

4.2 Robustness of the patterns

We investigated whether the results with the long NCEP reanalysis are consistent with the shorter reanalysis ERA, and whether the patterns depend on the period retained. Various tests were made which all suggest a weak dependence of the results outside the tropics on the period retained and on the particular product used. We will illustrate this by comparing NCEP with a reconstruction based on ERA P or *E-P* for the 1979/80–1992/93 winters. CCA modes are estimated from ERA P or *E-P* and NCEP SLP. This is then used for reconstructing *P* and *E-P* over the whole period of the NCEP data (winter 1958/59 to winter 1997/1998). The comparison is made separately for the period of ERA (winters 1979/80–1992/93) and the complementary period (1958–1979 and 1993–1997: non-ERA).

Trials have been made to obtain an optimal regression model by using in the CCA analysis 15 EOFs in precipitation and *E-P* fields which represent 75% and

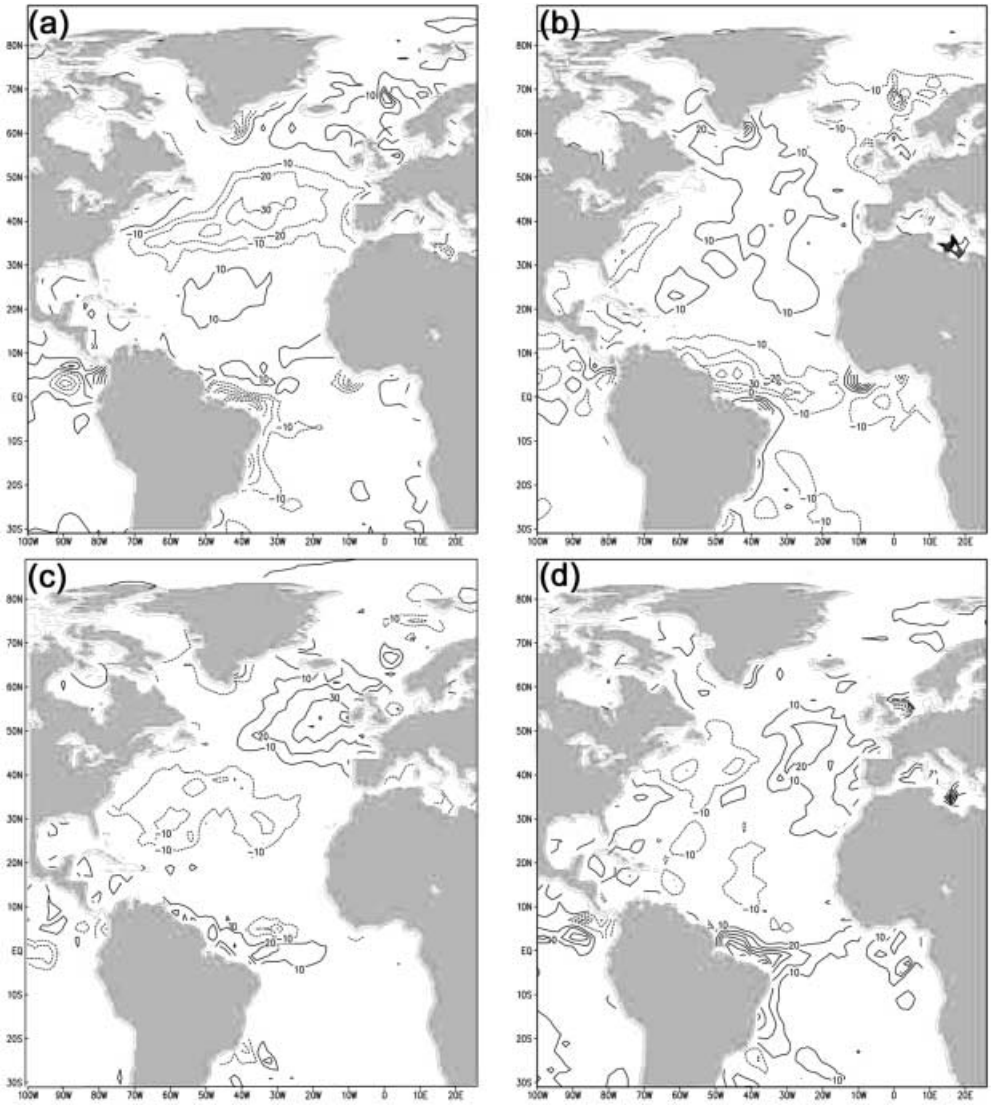

Fig. 2a–d First (**a**, **b**) and second (**c**, **d**) EOF of reconstructed precipitation and *E-P* (mm/month) for the winter months (1958–1998)

72% of the data variance respectively, and by varying the number of SLP EOFs and the number of CCA pairs. Only CCA modes with correlation coefficients higher than 0.50 have been considered in the regression models. The best regression models characterized by the highest correlation for the first two PCs of reconstructed and NCEP data for the ERA period are obtained using 5 CCA pairs for both *E-P* and *P* anomalies.

The correlation coefficients between the principal components of the reconstructed and NCEP *P* and *E-P* are illustrated in Table 2 for different regression models in the non-ERA period (first mode associated with NAO and second mode with EA). The corresponding first two EOFs are compared with the first two EOFs of NCEP precipitation and *E-P*. Both for the first and second EOF (Fig. 2), the patterns for reconstructed and NCEP data resemble each other as well as the CCA modes for NCEP described. The greatest differences are in the tropics where the magnitude of the variability is less pronounced in NCEP data than in the reconstructed field based on ECMWF reanalyses.

Correlation maps of the NCEP precipitation with the first and second PCs of reconstructed data using the best regression model are presented in Fig. 3 separately for winter months corresponding to the ERA and the non-ERA periods. For the main centres of action, correlation coefficients are statistically significant at a confidence level greater than 95%. The precipitation patterns correlated with the PCs (not shown) are similar for ERA and non-ERA intervals. This similarity between the two periods suggests that the NAO and EA related signals found in the precipitation field are not very sensitive to the actual period selected for building the model (here, based only on ERA-period data). For the *E-P* field (not shown), the correlations are rather less coherent than for *P* between the ERA and the non-ERA periods, but still display a great degree of similarity:

1. For the NAO EOF, the correlation pattern is relatively stable, especially over the Labrador Sea, the northeastern Atlantic and near the Iberian and northwestern African coasts
2. For the EA mode, the correlations between the second simulated principal component of *E-P* and either ERA or non-ERA NCEP *E-P* show a similar east/west anomaly contrast over the mid latitudes

The patterns related to NAO are more robust than the ones related to EA as the NAO features are better captured by the regression models than the EA features, even with a small number of retained EOFs and CCA pairs (see Table 2 for two EOFs and two CCA pairs).

The previous comparison is between model products. Although the two models and assimilation procedures are different, they could share similar biases. Therefore, we need also to compare the reconstruction of *P* and *E-P* which was just discussed with other products based on data. Correlation maps are first presented between the first two principal components of reconstructed data and *P*/*E-P* anomalies from a COADS-based gridded data set (Da Silva et al. 1994) for the winter months of 1976/77 to 1988/89. This is the period for which the data set is the most reliable. NAO and EA related signals are clearly present in these precipitation data (Fig. 4). All displayed correlation coefficients are statistically significant at a confidence level greater than 95%. The structure present in NCEP and ERA reanalyses (Figs. 1, 3) near the southern coast of Greenland is missing in the Da Silva data (1994) most likely due to poor observational coverage. Also, the correlation map for precipitation does not show the pronounced NAO-related subtropical centre of variability found in NCEP or in the reconstructed ERA data. The *E-P* correlation maps between the ship observations and the first two principal components of reconstructed data (not shown) are less coherent with the corresponding reanalyses and reconstructed patterns. Only the NAO related principal component reveals significant correlation coefficients, although it fails to reproduce the coastal feature near to North America present in both the ECMWF and NCEP data.

The Global Precipitation Climatology Project (GPCP) data (Huffman et al. 1996) and the Xie and Arkin (1997) composite products have been used to clarify the differences that are present in the tropical and subtropical areas. The results for GPCP (1988–1998, Fig. 5a, b) and for the Xie and Arkin product (1979–1998, Fig. 5c, d) are fairly similar and are consistent with the COADS results. They also exhibit a variability centre related to NAO near 15°S over South America.

Table 2 Correlation coefficient between the principal component (PCs) of NCEP precipitation and *E-P* with the PCs of reconstructed precipitation and *E-P*. Results for the first (*R*11) and second (*R*22) PCs are presented as a function of the number of EOFs of SLP retained for the CCA and the number of CCA pairs used in the reconstruction. Only the winter months from the intervals 1958–1979 and 1993–1997 (non ERA) have been used

Number of SLP EOFs		Number of CCA pairs		*R*11		*R*22	
Precipitation	*E-P*	Precipitation	*E-P*	Precipitation	*E-P*	Precipitation	*E-P*
2	2	2	2	−0.724	0.671	−0.381	−0.109
5	4	4	4	−0.726	0.782	0.632	0.621
6	6	5	5	−0.754	0.785	0.690	0.654
8	8	7	7	−0.508	0.424	0.200	−0.502

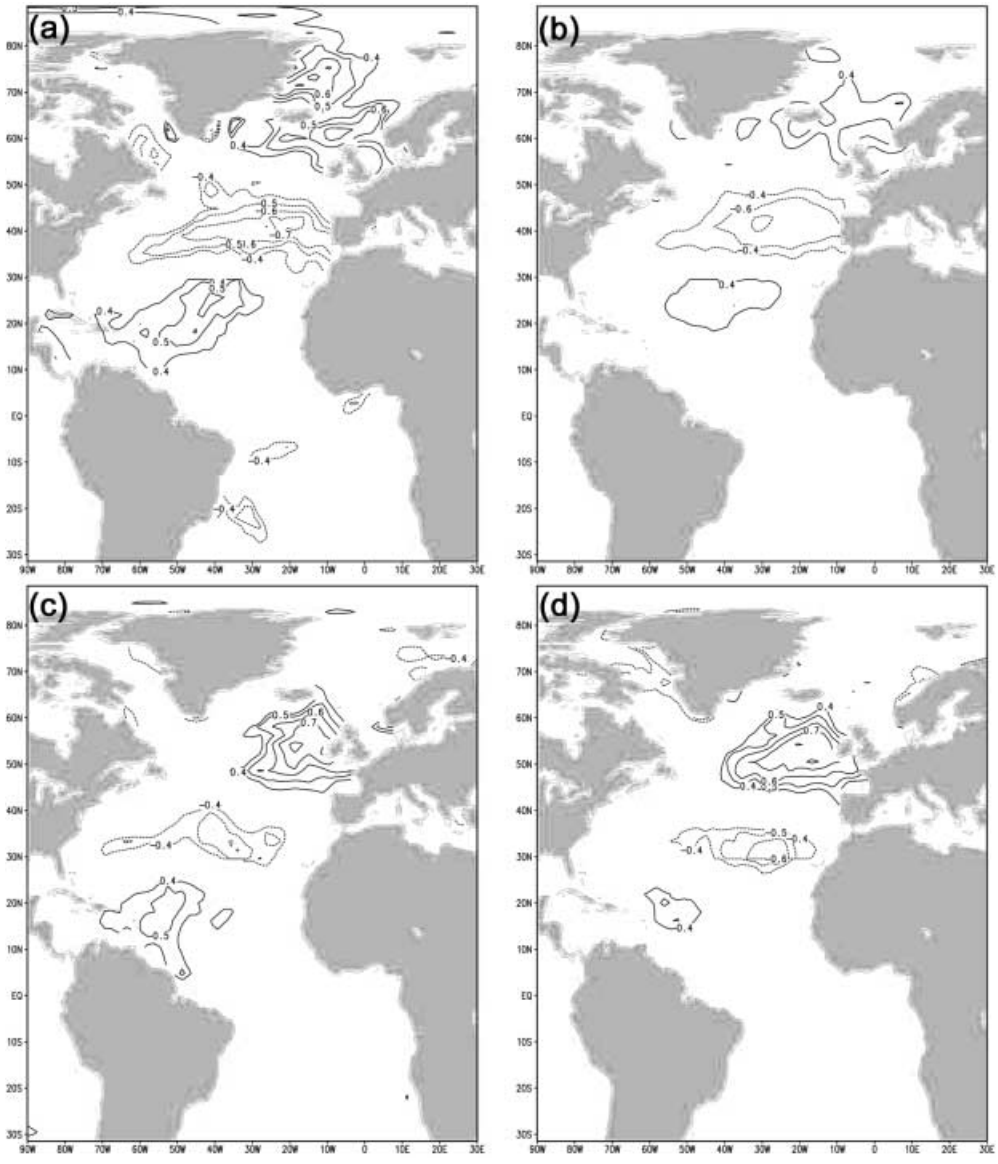

Fig. 3a–d Correlation coefficients of NCEP precipitation with the first and second principal components of simulated precipitation for **a, c** ERA and **b, d** non-ERA periods

The correlation coefficients are statistically significant at a level greater than 95% following Fisher's test for 30 pairs of time independent values ($R = 0.366$). The presence of this precipitation centre is also found in reconstructed and NCEP patterns (Figs. 2a, 3a) for the ERA period which overlaps the period of the other data sets.

4.3 Seasonal averages

NAO and EA related signals have been further investigated using winter averages (DJF) of monthly *E-P* and precipitation rate instead of individual months in order to filter residual high frequency variability. This results in more visible differences in the ITCZ area, with the first EOF in ERA precipitation and in *E-P* corresponding mainly to the ITCZ region, but absent in NCEP (not shown). The principal component associated with ERA shows a shift around 1988 which seems to be related to the Amazonian problem of the ERA experiment (Kållberg 1997) and the sudden African ITCZ displacement towards a 10° more southerly position after 1987 (Stendel and Arpe 1997). However, the NAO related pattern could still be identified in both reanalyses as the second mode (see Fig. 6 for its time series in ERA).

The same approach of reconstruction/validation is adopted as for the monthly averages. However, because of the problem in ERA, we use CCAs from NCEP *P*/*E-P* and SLP to identify patterns. The data set for the comparison with the reconstructed variability is now ERA (winters 1979/80 to 1992/93). Therefore to ensure a more stringent test on the robustness of the results, the CCA is made for the non-ERA period (26 winters from 1958/59 to 1977/78 and from 1993/94 to 1997/98). The reconstruction uses 15 EOFs of precipitation and *E-P* representing 85% and 83%, respectively, of the field

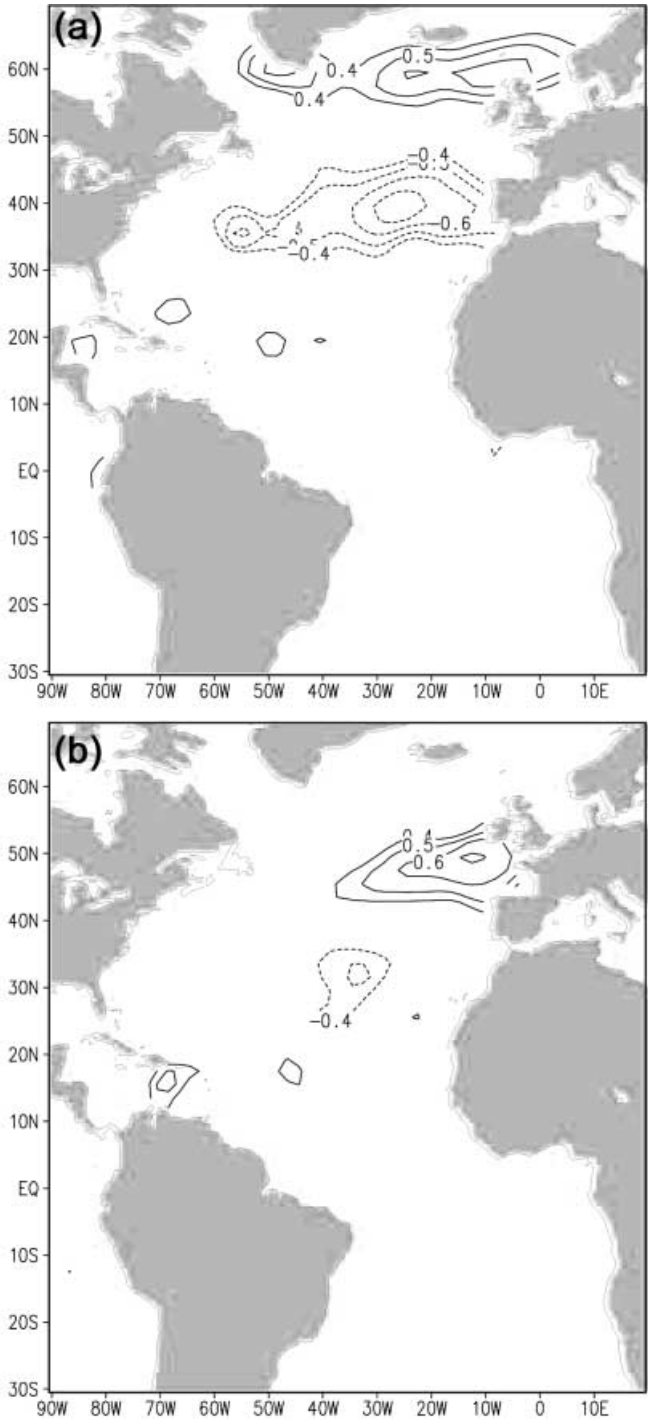

Fig. 4 Correlation coefficients between **a** first and **b** second principal components of reconstructed data and precipitation anomalies extracted from the Da Silva et al. (1994) data set for winter months in the interval 1976–1989

variance to obtain an optimum regression model by varying the number of SLP EOFs and CCA pairs. The correlation coefficients between the reconstructed and NCEP principal components associated with NAO and EA modes for different regression models are shown in Table 3.

When winter averages are used, only NAO related signals can be reconstructed, which is consistent with the very large share of the variance (67%) in the NAO mode for winter averaged data (EA mode only explains 13%). The best regression models characterized by the highest correlation between the first EOF of reconstructed data and the second EOF of ERA data use six CCA modes for precipitation and seven CCA modes for *E-P*. As can be seen in Table 3, the reconstruction is less successful for the freshwater flux. The principal components of reconstructed and ERA precipitation together are correlated with Hurrell's (1995) NAO index (Fig. 6) with a suggestion that ERA might be more correlated with the NAO index than the reconstructed field.

4.4 Annual averages

The annual averages have been computed from October to the next September and winter (DJF) means of SLP have been used to build the regression models. (At midlatitude, the annual SLP field is correlated to the winter average, and might be less relevant for a link to precipitation.) When these annual averages of *E-P* and precipitation rate are used, the reconstruction fails even when only data outside the tropics are considered and also when the reconstruction is for the ERA period. Although the highest correlation coefficient between the corresponding principal components of reanalysis and statistically reconstructed data is statistically significant, the correlation is small and the associated spatial patterns do not resemble each other. However, when we reconstruct precipitation and *E-P* from SLP without the constraint of reproducing the common features of NCEP and ERA variability, the NAO signal can still be identified. In this case, the reconstructed time series should be considered as filtered data rather than as reconstructed data. NCEP data from October 1958 to September 1979 and from October 1993 to September 1998 have been used as in the case of winter means of precipitation and *E-P* rates. We search for a regression model that correlates best the PCs of the reconstructed *P*/*E-P* with the first and the second principal components of SLP, for the validation interval 1979–1993. The model which uses three CCA pairs obtained from the first 15 EOFs of precipitation and three EOFs of SLP gives the highest correlation between the two principal components of reconstructed precipitation and NCEP SLP (0.988 for the first mode and 0.867 for the second one). The first mode (Fig. 7), explaining 56% of the reconstructed precipitation, resembles the NAO pattern which has been previously presented in the monthly (Fig. 2a) and winter average cases, but the correlation with the PCs of annual ERA precipitation is poor. The results (not shown) are not as good for the reconstructed *E-P*.

To check that this filtered result has some meaning, we consider spatial averages of NCEP annual precipitation in the main centres of action (based on an EOF

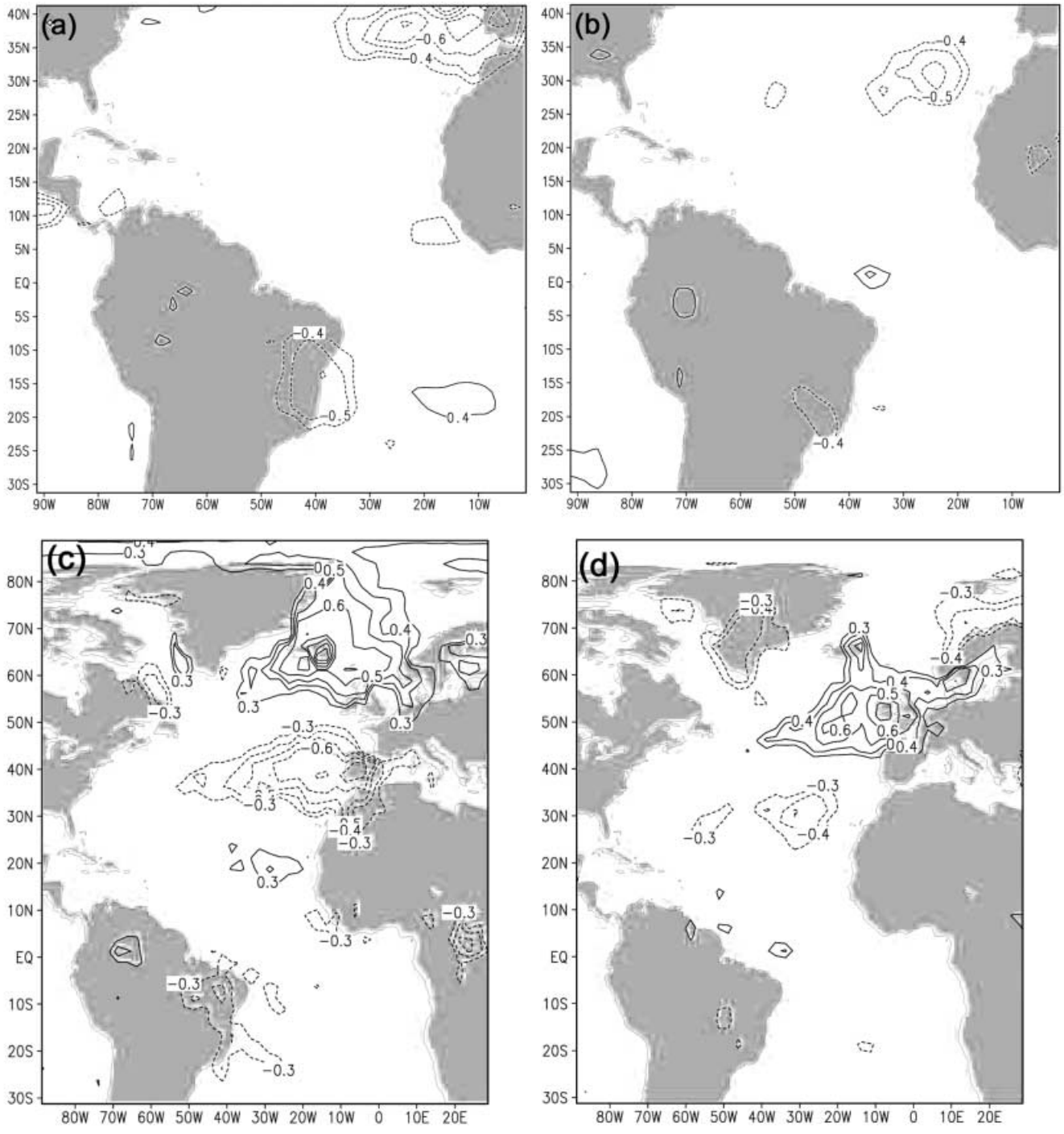

Fig. 5 Correlation coefficients between **a** first and **b** second principal components of reconstructed data and precipitation anomalies extracted from GPCP (Huffman et al. 1996) for the winter months 1988–1998; **c** and **d** correlations for first and second principal components with CPC (Xie and Arkin 1997) for the winter months 1979–1998

analysis), and correlation coefficients are computed between those averages and Hurrell's winter NAO index for October 1958–September1998. Not high but significant correlations at a level greater than 95% are found for the region from 30°N to 40°N in the eastern Atlantic (−0.43), in the Caribbean area (−0.49), in the eastern equatorial Atlantic (−0.43) and near the coast of northeast Brazil (0.37). The value in the Caribbean area is supported by observed negative correlation coefficients between the NAO index and the precipitation at Puerto Rico stations (Malmgren et al. 1998; Giannini et al. 2000). The analysis however suggests that on an interannual time scale other signals overwhelm the winter-NAO signals. This is not so surprising as we used a winter index, and the mid-latitude NAO index in other seasons is only weakly correlated with the winter

index. Also, in many areas, precipitation is not linked to the winter weather regimes that are more related to NAO. A major natural source of other variability on interannual time scales is ENSO related variability (Giannini et al. 2000). In addition, there is artificial noise due to the atmospheric model and data assimilation systems. The differences between NCEP and ERA suggest that this is particularly the case in the tropics of the Atlantic sector.

5 Discussion and conclusions

North Atlantic Oscillation (NAO) and Eastern Atlantic (EA) related signals have been found both in *E-P* and precipitation fields extracted either from ECMWF or NCEP reanalyses. They are more robust and stand the reconstruction test better for monthly averages than for the winter averages and even less so for annual averages, in particular for EA. In general, signals are better revealed and are more robust in the precipitation than in the freshwater (*E-P*) fields. There are indications that this results from the larger errors accumulated in freshwater flux from both precipitation and evaporation variables. Ocean fluxes computed in reanalysis experiments, in particular the evaporation, were found to be very sensitive to the data coverage (Kållberg 1997). Over large ocean areas there are few observations and this distribution varies in time. The acceptance and use of mismatched wind speed observations, whether they are erroneous or unrepresentative, lead to large variations in the surface fluxes (Kållberg 1997).

We encountered a different behaviour of NCEP and ECMWF variability in the tropical Atlantic (especially near the ITCZ), in particular on interannual time scales. Different mechanisms can be responsible for the relation between high and low latitudes in the NAO mode of ECMWF and NCEP reanalyses. The ERA patterns suggest a NAO signature in the tropical Atlantic which is strong in the monthly patterns and would indicate a link between the phase of NAO and changes in the position and intensity of the ITCZ. However, the analysis of winter rainfall based on satellite and in situ data (GPCP and CPC) does not support the monthly tropical pattern of ERA precipitation. They support, however, enhanced tropical variability for a NAO like mode in

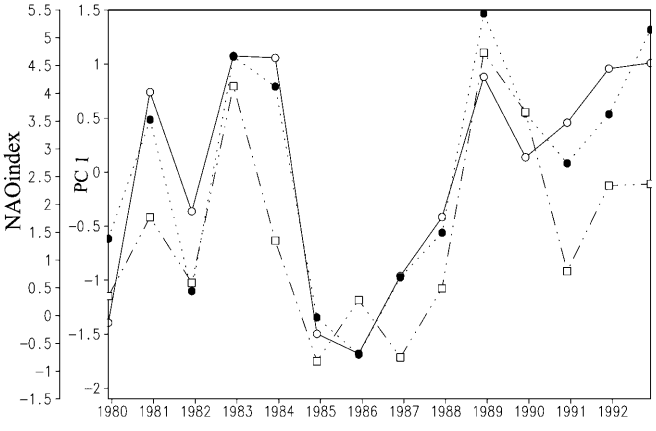

Fig. 6 First principal components of reconstructed precipitation based on NCEP data for non-ERA (*solid line*) and ERA (*dotted line*) winter averages, and the Hurrell (1995) NAO index (*dashed/dotted line*, *left scale*)

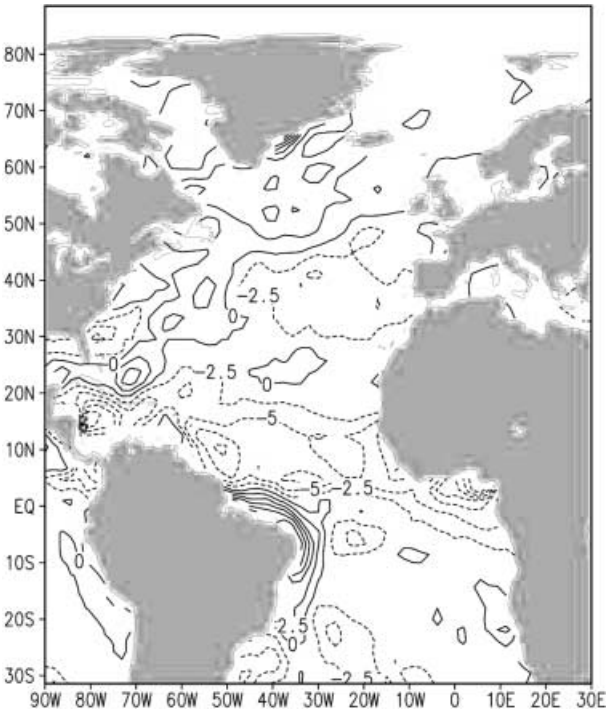

Fig. 7 The first EOF of reconstructed annual precipitation for the interval 1979–1993. Contours are in mm/month

Table 3 Correlation coefficient (*R*12) between the second principal component (PC) of ERA precipitation and *E-P* and the first PC of reconstructed precipitation and *E-P* for the winters 1979/80 to 1992/93. The correlation is presented as a function of the number of SLP EOFs retained for the CCA and of the number of CCA pairs used in the reconstruction

Number of SLP EOFs		Number of CCA pairs		*R*12	
Precipitation	*E-P*	Precipitation	*E-P*	Precipitation	*E-P*
2	2	2	2	0.810	−0.736
4	4	4	4	0.916	−0.747
7	7	6	6	0.920	−0.785
9	10	8	8	0.699	−0.759

reconstructed data from NCEP, and suggest a relation between convection near 15°S and NAO during northern winter. The tropical signal is consistent with other studies. Namias (1972) has presented evidence showing that the interannual variability of rainfall over northeast Brazil is related to the cyclonic activity in the Newfoundland-Greenland area and to fluctuations of the Azores high during the Northern Hemisphere winter. Malmgren et al. (1998) have shown that the fluctuations in annual precipitation at Puerto Rico are synchronous with the variations of winter NAO.

A number of observational and modelling studies have analyzed the role of heating in the tropical Atlantic for the Northern Hemisphere winter variability, suggesting that such a link to NAO is possible (e.g. Yang and Webster 1990; Watanabe et al. 1999; Robertson et al. 1999). For example, Yang and Webster (1990) suggest that the adjacent hemisphere heating is important in determining the location and magnitude of the westerly jet streams which in turn influence the winter variability modes such as NAO. However, based on observational and modelling evidence, tropical-extratropical linkage seems to be better identified on longer time scales (Bojariu 1997; Xie and Tanimoto 1998; Watanabe and Kimoto 1999; Rajagopalan et al. 1998) than on the month to interannual time scales that our analysis considers. This would be hard to identify in NCEP and ECMWF reanalyses, which are of limited reliability on those time scales. For instance, the position, intensity and seasonal cycle of ITCZ are rather uncertain in reanalyzed fields (Kållberg 1997; Stendel and Arpe 1997). Further analysis using observations and coupled ocean-atmosphere models is needed in order to clarify this issue.

In spite of these difficulties, the reanalyses obtained from two different models and assimilation systems (ECMWF and NCEP) usually show common modes of variability for very sensitive variables such as precipitation and E-P which gives hope that the reanalysis experiments can be used to further understand climate variability and carry out predictability studies. They should also be useful for investigating the impact on the upper ocean. The presence of a robust and stable NAO signal in the reanalyzed fields indicates that the study of NAO mechanisms and the analysis of the linkage between tropical and extratropical variability could benefit from the use of these detailed 3-dimensional data sets which are also temporally consistent. Our results indicate that it may be feasible to reconstruct past winter precipitation and E-P from the historical SLP fields, which are available for a much longer period (Kaplan et al. 1999), but this seems to be more difficult for the summer and annual averages.

Acknowledgements Grants from the Programme National de la Recherche du Climat were used to carry out this research. A "Poste Rouge" of the "Observatoire Midi-Pyrénées" supported two stays of Roxana Bojariu at LEGOS. This study was initiated when Gilles Reverdin was at LDEO (Palisades, New York) and was supported by NOAA grants 5-23175 and 5-61287. Comments by the reviewers and the editor were appreciated. This is Lamont-Doherty Earth Observatory contribution 6138.

References

Barnston A, Livezey RE (1987) Classification, seasonality and persistence of low frequency atmospheric circulation patterns. Mon Weather Rev 115: 1083–1126

Bretherton CS, Smith C, Wallace JM (1992) An intercomparison of methods for finding coupled patterns in climate data. J Clim 5: 541–560

Bojariu R (1997) Climate variability modes due to ocean-atmosphere interaction in the central Atlantic. Tellus 49A: 362–370

Busuioc A, von Storch H, Schnur R (1999) Verification of GCM-generated regional seasonal precipitation for current climate and of statistical downscaling estimates under changing climate conditions. J Clim 12: 258–272

Cayan DR (1992) Latent and sensible heat flux anomalies over the northern oceans: the connection to monthly atmospheric circulation. J Clim 5: 354–369

Cayan DR, Reverdin G (1994) Monthly precipitation and evaporation variability estimated over the North Atlantic and North Pacific. In: Atlantic Climate Change Programme: Proc PI's meeting, Princeton, May 9–11, 1994, 28–32

Curry RG, McCartney MS, Joyce TM (1998) Linking subtropical deep water climate signals to North Atlantic subpolar convection variability. Nature 391: 575–577

Cui M, von Storch H, Zorita E (1995) Coastal sea level and the large scale climate state. A downscaling exercise for the Japanese Islands. Tellus 47A: 132–144

Da Silva A, Young C, Levitus S (1994) Atlas of surface marine data 1994, Vol 1: algorithms and procedures. NOAA Atlas NESDIS 6, US Department of Commerce, Washington, D.C.

Dai A, Fung IY, Del Genio AD (1997) Surface observed global land precipitation variations during 1900–1988. J Clim 10: 2943–2962

Dickson RR, Meincke J, Malmberg S-A, Lee AJ (1988) The "Great Salinity Anomaly" in the northern North Atlantic 1968–1982. Prog Oceanogr 20: 103–151

Dickson RR, Meincke J, Rhines P, Swift J (1996) Long-term coordinated changes in the convective activity of the North Atlantic. Prog Oceanogr 38: 241–295

Frankignoul C, Czaja A, L'Hévéder B (1998) Air-sea feedback in the North Atlantic and surface boundary conditions for ocean models. J Clim 11: 2310–2324

Giannini A, Kushnir Y, Cane MA (2000) Interannual variability of Caribbean rainfall, ENSO, and the Atlantic Ocean. J Clim 13: 297–311

Gibson JK, Kallberg P, Uppala S, Hernandez A, Nomura A, Serrano E (1997) ERA Description, ECMWF Re-Analysis Project Report Series 1: 1–72

Hakkinen S (1999a) A simulation of thermohaline effects of a great salinity anomaly. J Clim 12: 1781–1795

Halliwell GR (1998) Simulation of North Atlantic decadal/multidecadal winter SST anomalies driven by basin-scale atmospheric circulation anomalies. J Phys Oceanogr 28: 5–21

Hauke H, Zorita E, Von Storch H (1996) Statistical downscaling of monthly mean North Atlantic air-pressure to sea level anomalies in the Baltic Sea. Tellus 48A: 312–323

Huffman GJ, Adler RF, PA, Rudolf B, Schneider U, Keehn PR (1995) Global precipitation estimates based on a technique for combining satellite-based estimates, rain gauge analysis, and NMP model precipitation information. J Clim 8: 1284–1295

Hurrell JW (1995) Decadal trends in the North Atlantic Oscillation: regional temperature and precipitation. Science 269: 676–679

Hurrell JW, van Loon H (1997) Decadal variations in climate associated with the North Atlantic Oscillation. Climate Change 36: 301–326

Kållberg P (1997) Aspects of the re-analysed climate. ECMWF Re-Analysis Project Report Series 2

Kalnay E, Kanamitsu M, Kistler R, Collins W, Deaven D, Gandin L, Iredell M, Saha S, White G, Woollen J, Zhu Y, Leetmaa A, Reynolds R, Chelliah M, Ebisuzaki W, Higgins W, Janowiak J, Mo KC, Ropelewski C, Wang J, Jenne R, Joseph D (1996) The NCEP/NCAR 40-Year Reanalysis Project. Bull Am Meteorol Soc 77: 437–471

Kaplan A, Kushnir Y, Cane MA (1989) Reduced space optimal optimal interpolation and historical marine sea level pressure. J Clim 12: 1854–1992

Kharin V (1994) The relationship between sea surface temperature anomalies and atmospheric circulation in general circulation model experiments. Max-Planck-Institut fur Meteorologie, Hamburg, Rep 136

Lazier JRN (1995) The salinity decrease in the Labrador Sea over the past thirty years. In: Martinson DG et al. (eds) Natural climate variability on decade-to-century time scales. National Academy Press, Washington, D.C. pp 295–302

Malmgren BA, Winter A, Chen D (1998) El-Nino-Southern Oscillation and North Atlantic Oscillation control of climate in Puerto Rico. J Clim 11: 2713–2717

Mauritzen C, Häkkinen S (1997) Sensitivity of thermohaline circulation to sea-ice forcing in an Arctic-North Atlantic model. Geophys Res Lett 24: 3257–3260

Namias J (1972) Influence of Northern Hemisphere general circulation on drought in northeast Brazil. Tellus 24: 336–342

Palmer TN, Sun Z (1985) A modelling and observational study of the relationship between sea surface temperature in the northwest Atlantic and the atmospheric general circulation. Quant J Roy Meteor Soc 111: 947–975

Preisendorfer RW (1988) Principal Component Analysis in meteorology and oceanography. Elsevier, Amsterdam

Rajagapolan B, Kushnir Y, Tourre YM (1998) Observed decadal midlatitude and tropical Atlantic climate variability. Geophys Res Lett 25: 3967–3970

Rahmstorf S (1995) Bifurcations of the Atlantic thermohaline circulation in response to changes in the hydrological cycle. Nature 378: 145–149

Robertson AW, Mechoso CR, Kim Y-J (2000) The influence of Atlantic sea surface temperature anomalies on the North Atlantic Oscillation. J Clim 13: 122–138

Rodwell MJ, Rowell DP, Folland CK (1999) Oceanic forcing of the wintertime North Atlantic Oscillation and European climate. Nature 398: 320–323

Rogers J (1990) Patterns of low frequency monthly sea level pressure variability (1899–1986) and associated wave cyclone frequencies. J Clim 3: 1364–1379

Rogers J (1997) North Atlantic storm track variability and its association to the North Atlantic Oscillation and climate variability of Northern Europe. J Clim 10: 1635–1647

Ropelewski CF, Halpert MS (1989) Quantifying Southern Oscillation-precipitation relationships. J Clim 9: 1043–1059

Schmittner A, Appenzeller C, Stocker TF (2000) Enhanced Atlantic freshwater export during El Niño. Geophys Res Lett 27: 1163–1168

Seager R, Kushnir Y, Visbeck M, Naik N, Miller J, Krahmann G, Cullen H (2000) Causes of Atlantic Ocean climate variability between 1958–1998. J Clim 13: 2845–2862

Stendel M, Arpe K (1997) Evaluation of the hydrological cycle in re-analysis and observations. ECMWF Re-Analysis Validation Reports – part 1. ECMWF Re-Analysis Project Report Series, 6

Tiedtke M (1993) Representation of clouds in large scale models. Mon Weather Rev 121: 3040–3061

van Loon H, Rogers CJ (1978) The seesaw in winter temperature between greenland and Northern Europe. Part I: General description. Mon Wea Rev 106: 296–310

von Storch H, Frankignoul C (1998) Empirical model decomposition in coastal oceanography. In: Brink KH, Robinson AR (eds) In the Sea, John Wiley and Sons, Vol 10, 47pp

von Storch H (1995) Spatial patterns: EOFs and CCA. In: von Storch H, Navarra A (eds) Analysis of climate variability: applications of statistical techniques. Springer, Berlin Heidelberg New York, pp 227–258

von Storch H, Zorita E, Cubasch U (1993) Downscaling of global climate change estimates to regional scales: an application to Iberian rainfall in wintertime. J Clim 6: 1161–1171

Wallace JM, Gutzler DS (1981) Teleconnection in the geopotential height field during the northern hemisphere winter. Mon Weather Rev 109: 784–813

Wallace JM, Smith C, Jiang Q (1990) Spatial patterns of atmosphere-ocean interaction in the northern winter. J Climate 3: 990–998

Watanabe M, Kimoto M, Nitta MT, Kachi M (1999) A comparison of decadal climate oscillations in the North Atlantic detected in observations and a coupled GCM. J Clim 12: 2920–2940

Welker GT, Bliss EW (1932) World Weather. V Mem Roy Meteor Soc 4: 53–84

Woodruff SD, Slutz RJ, Jenne RL, Steurer PM (1987) A comprehensive ocean-atmosphere dataset. Bull Am Meteorol Soc 68: 1239–1250

Xie P, Arkin PA (1997) Global precipitation: a 17-year monthly analysis based on gauge observations, satellite estimates, and numerical model outputs. Bull Am Meteorol Soc 78: 2539–2558

Xie P, Tanimoto Y (1998) A pan-Atlantic decadal climate oscillation. Geophys Res Lett 25: 2185–2188

Yang S, Webster PJ (1990) The effect of summer tropical heating on the location and intensity of the extratropical westerly jet streams. J Geophys Res 95: 18 705–18 721

Zorita E, Kharin V, von Storch H (1992) The atmospheric circulation and sea surface temperature in the North Atlantic area in winter: their interaction and relevance for Iberian precipitation. J Clim 5: 1097–1108